https://doi.org/10.59761/RCR5092

Applications of microwave technology in the field of solid oxide fuel cell — a review

Min Fu,[a] Xin Lin,[a] Xiangyang Li,[b] Zetian Tao[a]*

[a] *School of Resources, Environment and Safety Engineering, University of South China, Hengyang, Hunan Province 421001, China*
[b] *Decommissioning Engineering Technology Research Center of Hunan Province Uranium Tailings Reservoir, University of South China, Hengyang, 421001, PR China*

Microwave heating has gained considerable attention as a promising technology for the processing of ceramics, including materials used in solid oxide fuel cells (SOFCs). This unique heating method utilizes the dielectric loss of materials in an electromagnetic field, offering advantages such as rapid heating rates and low energy consumption. This review focuses on the recent applications and developments of microwave technology specifically for cathodes, anodes, and electrolyte materials in SOFCs. A deeper understanding of the potential benefits and challenges associated with microwave sintering can be gained by investigating the effects of microwave treatment on these SOFC materials. The ultimate goal of the review is to provide valuable insights into microstructure control and performance enhancement in SOFC materials through the use of microwave technology. By highlighting the advances and discussing the underlying mechanisms, researchers and practitioners in the field can explore the potential of microwave processing as a viable option for optimizing SOFC materials and improving overall cell performance.
The bibliography includes 106 references.
Keywords: SOFC, microwave sintering, cathodes, electrolytes, anodes.

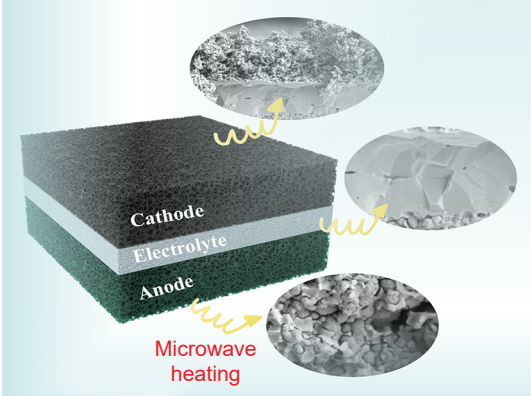

Contents

1. Introduction

Energy is a fundamental resource that exists in various forms, such as heat, electricity, light, mechanical energy, and chemical energy, among others. Over the past hundred years, fossil energy sources such as coal, oil, and gas have contributed significantly to the rapid development of the industrial economy.[1] However, the formation of fossil energy is a geological process that takes millions of years and cannot keep pace with the relentless and ever-increasing energy demands of modern humanity. What's more, most fossil energy is used through the combustion process, which generates a lot of harmful substances (such as dust, CO_2, NO_x, and SO_2) and causes serious environmental pollution.[2] Therefore, energy shortages and environmental pollution require a global shift to low-carbon and clean energy in the world.[3,4]

Fuel cells are electrochemical devices that convert chemical energy directly into electrical energy. These devices are not constrained by the Carnot cycle, which is one of the limitations of traditional chemical energy conversion methods.[5] In recent years, fuel cells have gained attention among many energy conversion technologies due to their remarkable efficiency (mainly related to cell size); versatility in application (used in both stationary power plants and portable power devices); as well as their sustained power output and low pollutant emissions.[6,7] Among the many types of fuel cells, the solid oxide fuel cell (SOFC) is environmentally friendly due to its solid electrolyte, which avoids corrosive environments and facilitates assembly.[8,9]

The current trend in SOFC application is to operate at medium (800 °C) to low (500 °C) temperatures, which places higher demands on the material preparation process. In high-temperature (⩾ 900 °C) operation, SOFCs exhibit advantageous characteristics such as reduced polarization losses, and are not

M.Fu. Master (doctor), Student.
X.Lin. Bachelor, Student.
X.Li. Doctor, Professor.
Z.Tao. Doctor, Professor.
E-mail: newton@mail.ustc.edu.cn; taozetian@usc.edu.cn
Current research interests of the authors: solid oxide fuel cells.

Received 19 June 2023

dependent on the use of precious metals as electrode catalysts. However, there are problems such as grain coarsening and reduced electrode porosity, resulting in reduced electrode activity.[10,11] In addition, the inter-diffusion or reaction between the electrolyte and the electrode creates a highly resistive phase that leads to a reduction in the ionic conductivity of the electrolyte.[12] Therefore, achieving lower operating temperatures is one of the key issues to reduce production costs and promote the commercialization of SOFCs.

Microwave heating technology, with its rapid heating and high efficiency, is considered by researchers to be a new environmentally friendly technology.[13–16] Since the 1940s onwards, it has been discovered that electromagnetic waves with frequencies ranging from radio frequency to the microwave band can also heat materials, especially in many areas where microwave heating has characteristics that are incomparable to traditional heating methods. Microwave heating, unlike more traditional heating methods, does not rely on heat transfer but rather on the conversion of electromagnetic energy into thermal energy. The interaction mechanism between the material and the electromagnetic wave plays a crucial role in the process of microwave heating, as it directly influences the efficiency of converting electromagnetic energy into thermal energy.[17–19] It has the following additional advantages over the conventional heating techniques, including:

Homogeneous rapid heating that heats an object by microwave absorption.

Selective heating occurs as a result of the special dielectric properties of various components of the cell materials.

The use of cleaner energy sources and the implementation of cleaner heating processes with the reduction of secondary waste.

Recently, microwave heating technology has been widely used for the preparation and optimization of functional ceramic materials due to its unique ability to homogenous sintering, providing a uniform microstructure, and excellent mechanical performance. The synthesis of $Na_3Zr_2Si_2PO_{12}$ (NZSP) solid electrolytes by rapid low-temperature microwave sintering has been reported.[20] Microwave-assisted solid phase reaction method was then confirmed to increase the ionic conductivity of NZSP electrolytes.[21] In addition, rapid microwave sintering has been used to process functional electro-ceramic materials. The possibility of tailoring their microstructure and functional properties by selecting rapid microwave sintering regimes has also been discussed.[22] Furthermore, the microwave sintering technique has recently been demonstrated in a significant number of experiments to be able to selectively control the microstructure of ceramic materials, thus realizing the manipulation of performance.[23–26]

Intensive research has been devoted to exploring the application of microwave heating to improve the properties of SOFC materials.[27] Recently, Yu published a review focusing on the densification of electrolyte precursors in SOFCs by microwave heating technology.[28] As shown in Fig. 1, various components of SOFC systems, including anodes, cathodes, and electrolyte-based materials, have been investigated under microwave conditions. These studies have focused on understanding the effects of microwave treatment on microstructure, conductivity, activation energy, and electrochemical properties. In particular, the conductivity, activation energy, and electrochemical performance of the materials are all affected by their microstructure. Figure 2 gives an overview of the influence of the microwave-assisted processes on the grain size of the materials. Microwave-assisted techniques have been observed to increase the grain size and density of

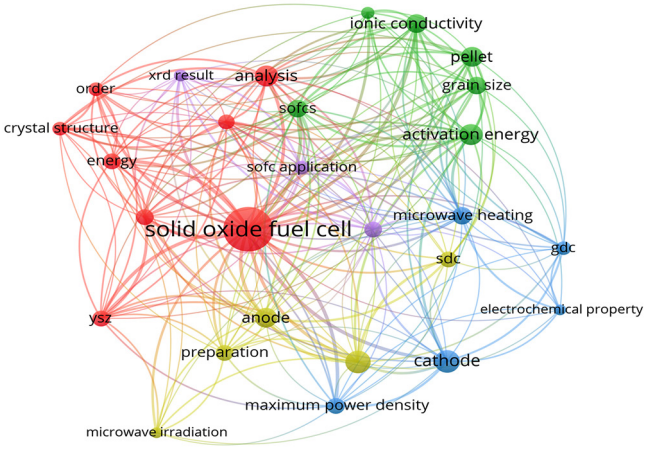

Figure 1. Schematic of published topics related to microwave heating effects on SOFC properties.

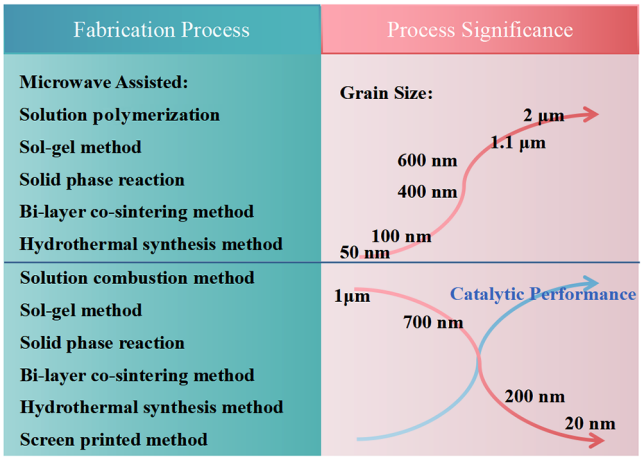

Figure 2. An overview of the influence of the microwave-assisted processes on the grain size of the materials.

electrolyte materials. Conversely, for anode and cathode materials, microwave-assisted methods often result in nanoscale grain sizes. Despite the considerable researches that have been conducted on microwave treatment of fuel cell materials, a comprehensive summary of key findings is still lacking. Therefore, in order to present the progress made in this field, it is essential to provide a systematic review of the work to date and to enable the readers to gain insight into future research directions.

This research aims to showcase the possible applications of microwave technology in the fuel cell industry by analyzing the microwave sintering mechanism and outlining the modifications in the key components of the fuel cell system, such the electrolyte, cathode, and anode.

2. Microwave heating mechanism

The mechanism of microwave heating reflects the conversion of electromagnetic energy into thermal energy that occurs at the atomic level in a material placed in the electromagnetic field of a microwave device. The dielectric properties of a material determine its ability to absorb electromagnetic field energy.[29] The study of microwave thermal processes requires a thorough understanding of the correlation between material properties and

the value of microwave electromagnetic energy. The efficiency of absorption of microwave energy is determined by the properties of the material, which can change as the energy is absorbed, so the properties of the material change in a controlled manner depending on the time the material is in the electromagnetic field.[30–32]

The advanced ceramic materials, especially new materials for solid oxide fuel cells, are generally composite or multi-phase materials, which are consequently hybrid absorbers. Currently, microwave technology is utilized for the processing of ceramic matrix composites (CMC), which primarily comprise a reinforcement phase and a matrix phase. The microwave processing of CMC is influenced by several of critical factors, including the microwave frequency, the dielectric characteristics of the base and reinforcing materials, the critical temperature at which the ceramic can be susceptible to the microwave energy, and the particle size of the material.[33] Ceramic molecules interact weakly with electromagnetic waves due to their relatively low dielectric properties. Consequently, many ceramic materials possess a high degree of transparency to microwave radiation under normal environmental conditions. However, above certain critical temperatures (for example, above 600 °C for alumina), the material's dielectric properties rapidly increase, resulting in effective heating. During the processing of CMC, reinforcing materials with high dielectric loss factors (*e.g.* SiC, zirconium oxide) can be added to the matrix with low dielectric loss factors (*e.g.* Al_2O_3, SiO_2, Fe_3O_4).[34,35] Reinforcing materials with a high dielectric loss factor work as a high energy source in a ceramic matrix with a low loss factor due to the absorption of microwave energy.

A schematic representation of the microwave mechanism is shown in Fig. 3 *a*,*b*. The CMC is initially heated by a hot spot in the reinforcement powder by conventional heat transfer until the temperature of CMC reaches a critical temperature. After the critical temperature, microwave energy can be coupled with both matrix and reinforcement powder, resulting higher densities through uniform heating mechanism. As the powder size of CMC and reinforcement decreases, the mechanical properties can be improved through microwave heating, as shown in Fig. 3 *c*.

3. Preparation of SOFC materials by microwave heating

3.1. Electrolyte materials

The electrolyte, which separates the gases used for the fuel and air electrodes to prevent efficiency loss or cell failure due to gas leakage, is a critical component of a solid oxide fuel cell. It acts as a conductor of oxygen/proton ions to create a circuit between the fuel and air electrodes. As a result, the electrolyte material must meet the following criteria: (1) high oxygen ion conductivity and electron nonconductivity; (2) high densities to isolate the reactive gases in the porous layer on both sides; (3) excellent redox stability; (4) good thermal cycling stability and mechanical strength; and (5) good chemical compatibility with electrode materials and sealing materials, and have a thermal expansion coefficient that matches to the coefficients of these materials to prevent delamination.

The unique advantages of microwave sintering technology for producing dense electrolyte layers have been demonstrated in several publications. The initial scholarly investigation of the microwave heating of dense ceramics was carried out on the composition $La_{0.8}Sr_{0.2}Ga_{0.83}Mg_{0.17}O_{2.815}$ (LSGM).[37] The study revealed that the synthesis and sintering of LSGM using microwave heating could be achieved in a surprisingly short time of 10 min. In this process, sodium '*β*' alumina was used as the receiver of microwave energy, resulting in the formation of LSGM with 94% density. It should be noted that the samples obtained by microwave heating had a smaller grain sizes and lower conductivity than those sintered by the conventionally method. According to Fig. 4, the average grain size of the microwave sintered sample was 4 μm, while for the conventionally sintered sample that was approximately 10 μm. Rambabu *et al.*[38] then investigated the effect of conventional

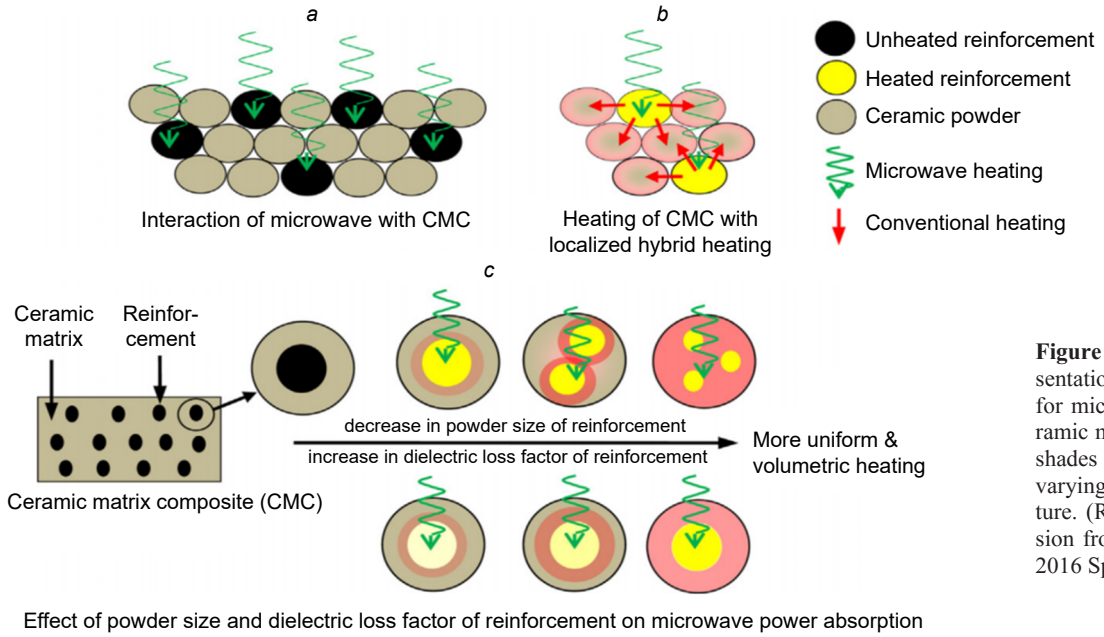

Figure 3. Schematic representation of the mechanism for microwave heating of ceramic matrix composites. The shades of rose balls indicate varying degrees of temperature. (Reprinted with permission from Ref. 36. Copyright 2016 Springer Link.)

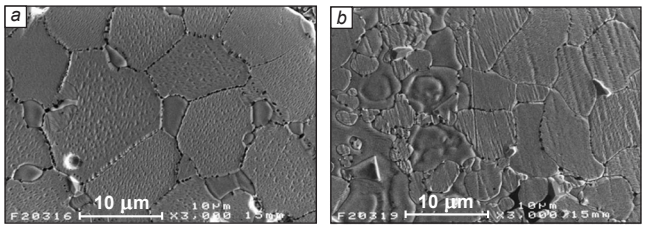

Figure 4. Scanning electron microscopy (SEM) images of LSGM ($La_{0.8}Sr_{0.2}Ga_{0.83}Mg_{0.17}O_{2.815}$) samples obtained by: (*a*) conventionally sintered at 1793 K in air for 12 h; (*b*) microwave sintered for 10 min. (Reprinted with permission from Ref. 37. Copyright 2003 Springer Link.)

and microwave-assisted sintering on recycled LSGM samples obtained by the 'regenerative' sol-gel (RSG). The RSG method is a combination of the solid state reaction and the Pechini-type method. According to the research results, microwave heating has been shown to be a technology that offers advantages in terms of both time and cost efficiency for the preparation of LSGM electrolyte materials. Zhai *et al.*[39] reported another refined method to obtain a smaller grain size (2–3 μm) of LSGM by microwave. So far, microwave heating technology has shown advantages in the producing even smaller grain sizes. Subsequently, microwave heating technology was used to produce homogeneous nanoparticles of ceria powders with a grain size 28% smaller than that of conventional commercial ceria, as shown in Fig. 5.[40]

The unique advantages of microwave sintering technology in improving the electrochemical properties of electrolytes have also been demonstrated in several studies. In order to suppress electronic conductivity, microwave heating has been used as a superior energy saving source while successfully producing

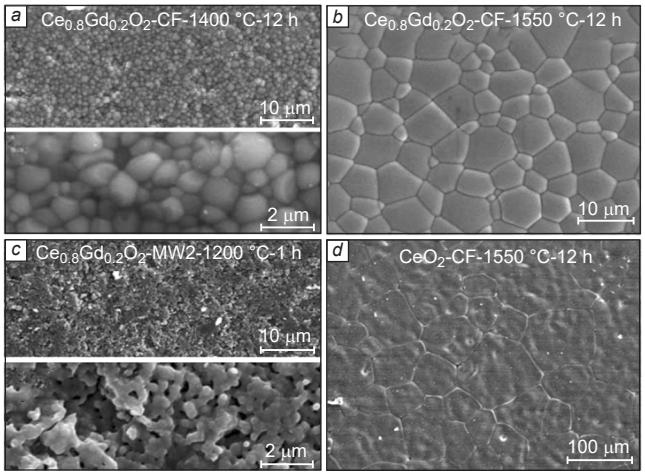

Figure 5. SEM images of the ceria pellets obtained by heating: (*a*) at 1400 °C for 12 h in a resistance furnace; (*b*) and (*d*) at 1550 °C for 12 h in a resistance furnace; (*c*) at 1200 °C for 1h in microwave oven. (Reprinted with permission from Ref. 40. Copyright 2006 Springer Link.)

electron trapping nanoparticals[41]. Wang *et al.*[42] reported microwave heating behaviors of four different compositions of yttria-stabilized zirconia (YSZ) electrolyte materials. It can be concluded that the microwave field is well coupled to the YSZ electrolyte, allowing for faster and more homogeneous crystallization. In order to reduce the ohmic resistance of SOFCs, Jiao *et al.*[43] developed an effective and simple method (slurry spraying followed by microwave heating) to reduce the electrolyte film of YSZ to less than 10 microns, thus extending the microwave heating technology from the preparation of the electrolyte film to the treatment of the whole cell.

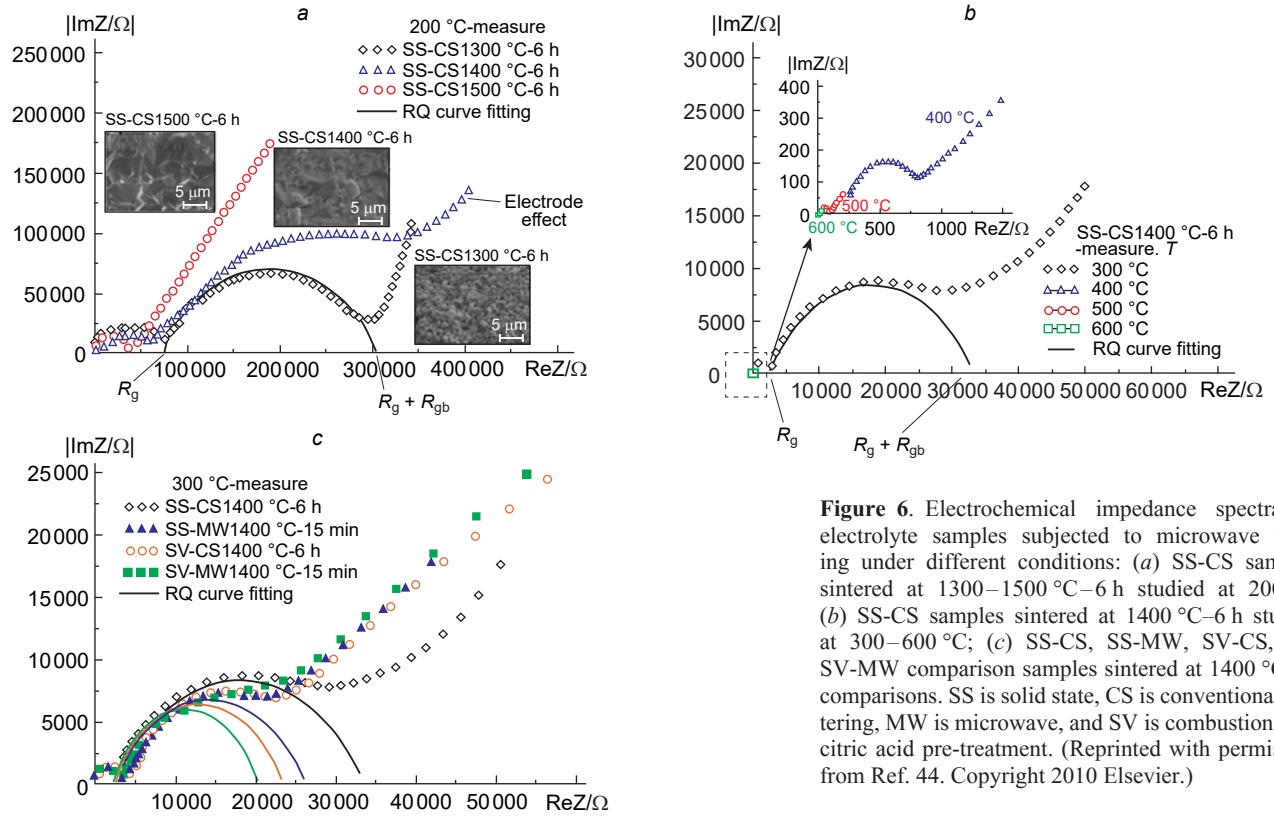

Figure 6. Electrochemical impedance spectra of electrolyte samples subjected to microwave heating under different conditions: (*a*) SS-CS samples sintered at 1300–1500 °C–6 h studied at 200 °C; (*b*) SS-CS samples sintered at 1400 °C–6 h studied at 300–600 °C; (*c*) SS-CS, SS-MW, SV-CS, and SV-MW comparison samples sintered at 1400 °C for comparisons. SS is solid state, CS is conventional sintering, MW is microwave, and SV is combustion with citric acid pre-treatment. (Reprinted with permission from Ref. 44. Copyright 2010 Elsevier.)

Among the factors affecting the performance of SOFCs, the microstructure of the electrolyte plays a crucial role and often depends on the powder preparation methods. The effect of microwave rapid sintering on the grain boundary resistance and grain resistance of the electrolyte (multiple-element doped ceria-based electrolyte) has been investigated.[44] As shown in Fig. 6 *a*), the grain boundary resistance decreases with increasing grain size, while the grain size increases with increasing sintering temperature increases. It has been noted that grain boundary resistance can be decreased at lower temperature of the process (as shown in Fig. 6 *b*). In addition, the grain boundary resistance of microwave heated samples is relatively small at 300 °C (as in Fig. 6 *c*), which may be due to segregation of amorphous and dopant phases, or local defects caused by space charge effects. Rapid microwave co-sintering of anode-electrolyte was investigated by Jiao *et al*.,[45] who showed that microwave heating can be used for rapidly producing dense YSZ electrolyte films and to improve cell performance improved by 16%. Subsequently, Acharya[46] found that the grain size growth rate for the microwave sintered electrolyte was linearly related to the rapid densification of the electrolyte film. Smaller grain size was produced by microwave sintering at lower temperatures, resulting in faster oxygen ion conductivity at the grain boundaries. SDC ($Ce_{0.8}Sm_{0.2}O_{19}$) electrolytes with smaller grain sizes were determined by rapid microwave sintering, and their ionic conductivity and activation energy were refined as electrochemical impedance spectroscopy shown.[47] Gadolinium doped ceria electrolyte (GDC, $Ce_{0.9}Gd_{0.1}O_{1.95}$) was synthesized by microwave coupled heating, demonstrating the great influence of microwaves on the morphology of GDC and consequently on the electrical conductivity of the electrolytes.[48]

Recent researches on electrolyte membrane materials for SOFCs have focused on high ionic and negligible electronic conductivity at intermediate temperatures. However, the sinterability of these materials is poor.[49–52] Microwave hybrid heating can overcome the difficulty of electrolyte densification. Silicon carbide exhibits susceptibility to electromagnetic wave coupling and is sensitive to rapid heating due to dielectric loss effects. As a result, the electrolyte can be efficiently heated by conventional heat transfer from the silicon substrate. Santos *et al*.[53] reported that the successful fabrication of $La_{9.33}Si_2Ge_4O_{26}$ materials by silicon carbide-assisted microwave hybrid heating at a lower temperature. The microwave-heated polycrystalline powder $Ce_{0.8}Sm_{0.18}Ca_{0.02}O_{1.9}$ has promising properties as a potential material for mediate temperature SOFCs. This is due to its suitable properties, including low grain boundary resistance and enhanced ionic conductivity.[54] Figure 7 shows the dependence of the grain size of electrolyte materials on the duration of microwave heating, which can be used to control the oxygen-ion conductivity of the material.

It is well known that microwave heating differs from conventional heating in that it relies on the dielectric loss of the material to convert electromagnetic energy into thermal energy. This means that the dielectric properties of the material determine its microwave sintering performance. Various researchers have used materials with high dielectric properties to assist in microwave sintering of materials with low dielectric properties. Solid oxide fuel cells researchers are no exception. To improve the microwave sintering performance of gadolinium doped ceria electrolytes, Hari *et al*.[55] investigated a novel method to prepare nanopowder of Li-GDC with lithium nitrate salt added as a microwave sintering aid. The Li doping, not only acted as a microwave sintering aid to reduce the sintering temperature of the GDC to 600 °C, but also resulted in a 6-fold increase in grain size. Abdullah *et al*.[56] reported that the conductivity value of GDC or Sm-doped CeO_2 (SDC) sintered under millimeter-wave irradiation heating was higher than under conventional heating. The design of their invention conductivity tester is shown in Fig. 8. Jais *et al*.[57] investigated the properties of zirconia co-doped with 10 mol.% Sc and 1 mol.% Ce (scandia–ceria–stabilized–zirconia, 10Sc1CeSZ) electrolyte synthesized by the microwave-assisted glycine nitrate method. The conductivity is the highest reported for this class of

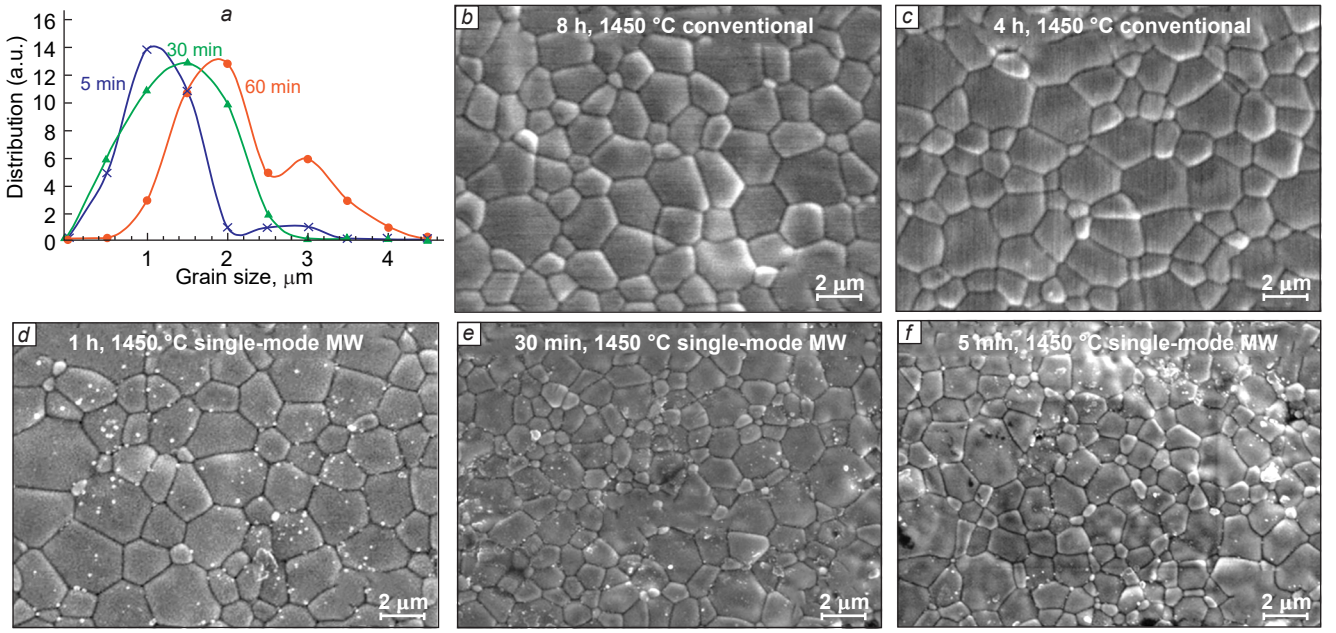

Figure 7. (*a*) Grain size distribution of $Ce_{0.8}Sm_{0.18}Ca_{0.02}O_{1.9}$ as a function of microwave heating time. SEM micrographs for the samples obtained by heating under different conditions; (*b*) conventional heating, 8 h, 1450 °C; (*c*) conventional heating, 4 h, 1450 °C; (*d*) microwave heating, 1 h, 1450 °C; (*e*) microwave heating, 30 min, 1450 °C; (*f*) microwave heating, 5 min, 1450 °C. (Reprinted with permission from Ref. 54. Copyright 2015 Elsevier.)

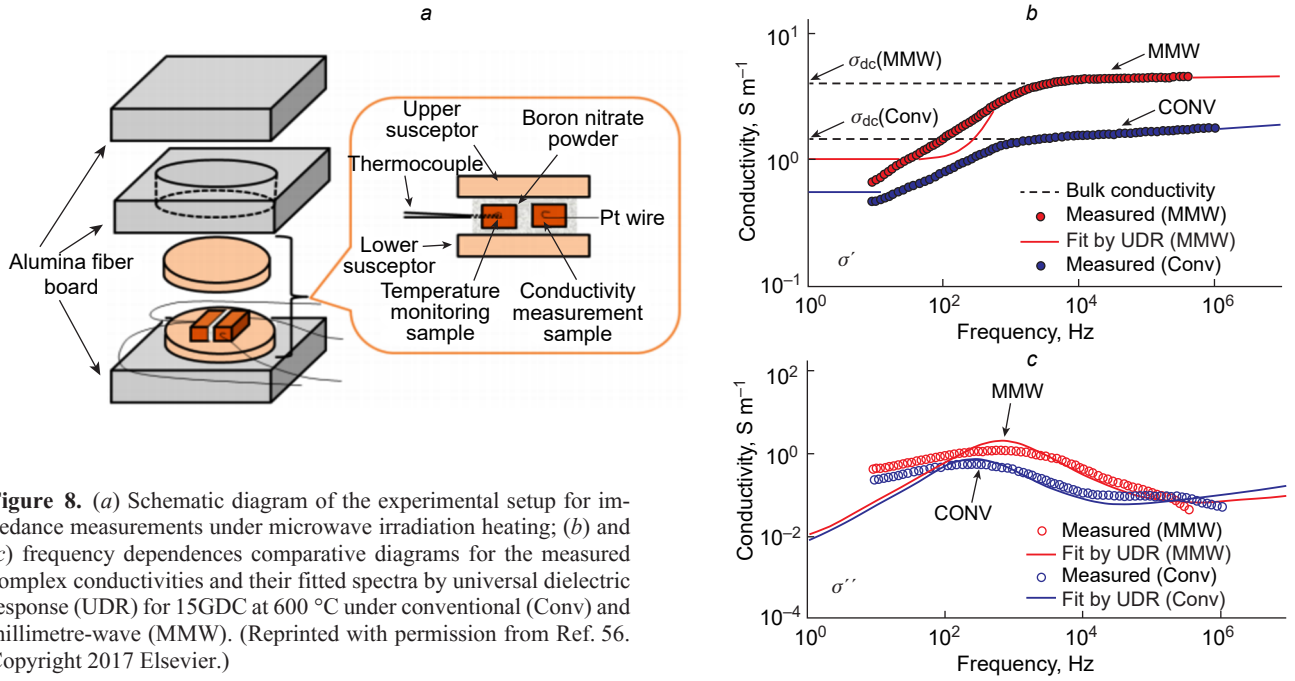

Figure 8. (*a*) Schematic diagram of the experimental setup for impedance measurements under microwave irradiation heating; (*b*) and (*c*) frequency dependences comparative diagrams for the measured complex conductivities and their fitted spectra by universal dielectric response (UDR) for 15GDC at 600 °C under conventional (Conv) and millimetre-wave (MMW). (Reprinted with permission from Ref. 56. Copyright 2017 Elsevier.)

electrolyte, indicating the potential of microwave-induced powders for the development of electrolyte materials.

Nevertheless, doped cerium-based electrolyte materials usually suffer from unsatisfactory open circuit voltage (OCV).[58–61] Ce^{4+} in ceria can be easily reduced to Ce^{3+} in reduced atmosphere at elevated temperatures. The reduction behavior has the potential to cause both mechanical degradation of the electrolyte as a result of crystal lattice expansion and the induction of n-type electrical conduction inside the electrolyte. The conduction behavior of the n-type material leads to a partial internal short circuit, which subsequently causes a significant reduction in the OCV of a fuel cell. Kumar *et al.*[62] prepared the samarium doped barium cerate based $Ce_{0.8}Sm_{0.2}O_{2-\delta}$–$BaCe_{0.8}Sm_{0.2}O_{3-\delta}$ (SDC–BCS) based composite electrolyte by wet chemistry method and microwave sintering. High ionic conductivity is achieved for composite electrolytes microwave sintered at 1400 °C for 20 min. The increase in conductivity is due to the diffusion of oxygen ions migrating mainly through the continuous channels of the second phase (samarium doped barium cerate). The co-dopant composition $Ce_{0.85}La_{0.075}Sm_{0.075}O_{2-\delta}$ was synthesized by hydrothermal method and sintered in cylindrical pellets form by rapid microwave sintering[63]. Madhusudan *et al.*[64] investigated the Dy and Pr co-doped ceria $Ce_{0.8}Pr_{0.2-x}Dy_xO_{2-\delta}$ as electrolyte material by microwave-assisted sol-gel method, obtaining highest total ionic conductivity of 6.8×10^{-3} S cm^{-1} and minimum activation energy of 0.80 eV at 500 °C for the case where x equals 0.1. Furthermore, tri- or multi-doped ceria was investigated because single-doped ceria has disadvantages such as reduced cerium content, low oxygen partial pressures, and electronic conductivity. Raman spectroscopy results revealed that the samples $Ce_{0.8}Sm_{0.1}Y_{0.1}O_{2-\delta}$ and $Ce_{0.76}Pr_{0.08}Sm_{0.08}Gd_{0.08}O_{2-\delta}$ exhibit an increased concentration of oxygen vacancies, which in turn leads to improved ionic conductivity.[65,66]

Utilizing microwave sintering technology to prepare SOFCs not only increases the electrolyte's density but also modifies the cathode-electrolyte interface, thus decreasing the polarization resistance and ohmic resistance.[67] The microwave co-sintering method was also used to produce bi-layer of BCZY ($BaCe_{0.7}Zr_{0.1}Y_{0.2}O_{3-\delta}$) and NiO-BCZY at 1200 °C.[68] According to the study by Xu, microwave sintering could improve the protonic conducting performance of BZCY.As shown in Fig. 9 *a*,*b*, the X-ray diffraction (XRD) technique was used to compare the phase purity of the BCZY electrolyte that obtained by microwave sintering and conventional sintering. The results revealed the existence of a pure BZCY phase obtained by microwave sintering, without any detectable impurities. Whereas the BZCY material obtained via conventional sintering showed the existence of Y_2O_3 heterogeneous phase. It was reported that the elevated temperature leads to the vaporization of barium oxide, resulting in the occurrence of A-site defects within the lattice structure.[69] Consequently, this phenomenon was shown to be a trigger for the production of Y_2O_3. The microscopic size of Y_2O_3 heterophase limits the proton conduction (see in Fig. 9 *c*). This explains why the microwave sintered BZCY electrolyte has a higher proton conductivity.

In summary, microwave technology offers unique advantages in the preparation of electrolyte materials, resulting in optimized electrochemical properties. Table 1 highlights the key areas of microwave heating application, which include microwave-assisted electrolyte powder synthesis and the preparation of layers of dense electrolytes. Numerous studies shown that the lattice size of microwave-assisted synthesized electrolyte powders, such as oxygen ion conductors and proton conductors, tends to be at the nanoscale level. This nanoscale morphology of the electrolyte powders was found to affect their electrochemical properties. By taking advantage the benefits of microwave technology; researchers can achieve finer control over the microstructure and performance of electrolyte materials in solid oxide fuel cells.

3.2. Anode materials

The anode is a critical component of the SOFCs because it facilitates the catalytic oxidation reaction of the fuel. For efficient fuel oxidation, the anode material must have high catalytic activity and a large specific surface area. Currently,

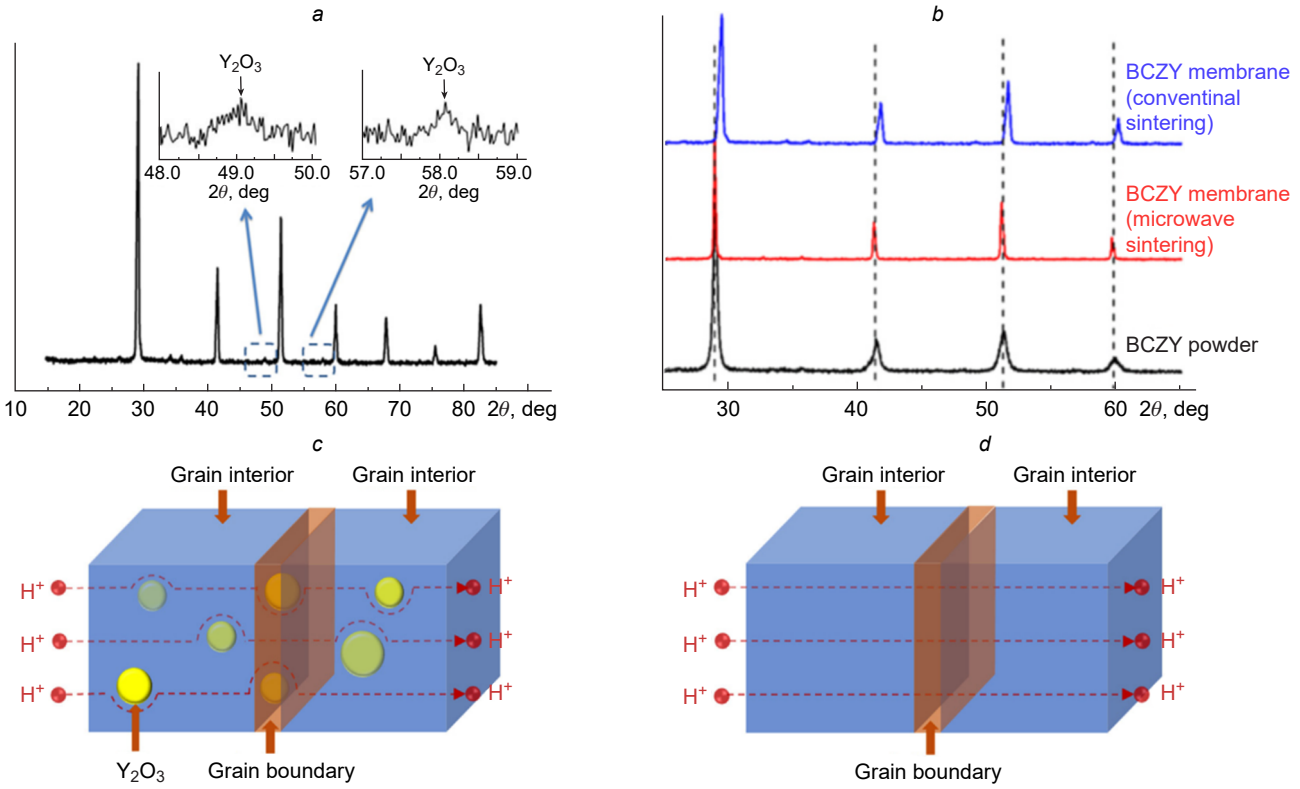

Figure 9. (*a*) X-ray diffraction (XRD) pattern for the BCZY membrane prepared by the conventional sintering method; (*b*) comparative XRD patterns of BCZY powder prepared by different methods; schemes of proton transport through the BCZY membrane prepared by (*c*) conventional sintering method and (d) microwave sintering method. (Reprinted with permission from Ref. 68. Copyright 2018 Elsevier.)

Table 1. A brief summary of microwave assisted preparation of electrolyte membrane materials.

Membrane electrolyte	Fabrication process	Grain size	Microwave processing	Electrochemical properties	Ref.
$La_{0.8}Sr_{0.2}Ga_{0.83}Mg_{0.17}O_{2.815}$	MW assisted solution polymerization	2–3 μm	1400 °C, 9 h	–	37
$Gd_{0.2}Ce_{0.8}O_{1.9}$-0.34Mn-0.34Co-Al_2O_3	MW assisted sol-gel method	–	1350 °C, 30 min	–	41
$(La_{0.75}Sr_{0.2}Ba_{0.05})_{0.175}Ce_{0.825}O_{1.891}$	MW assisted combustion	2 μm	1400 °C, 15 min	$\sigma_{600\ °C} = 10^{-2}$ S cm^{-1}	44
$Ce_{0.8}Gd_{0.2}O_{1.95}$	MW assisted combustion	0.5–2 μm	170 °C, 2 h		70
YSZ	MW assisted anode-electrolyte co-sintering process	2–3 μm	1600 °C	0.4 W cm^{-2} (800 °C)	45
$Ce_{1-x}Dy_xO_{2-x/2}$ (x = 0.05–0.25 at.%)	MW assisted synthesis and sintering	400 nm	1050 °C, 1 h	$\sigma_{550\ °C} = 7.42 \times 10^{-2}$ S cm^{-1}	46
$La_{9.33}Si_2Ge_4O_{26}$	MW assisted solid phase synthesis	–	1350 °C, 1 h	–	71
$Sm_{0.2}Ce_{0.8}O_{1.9}$	MW assisted sol-gel method	100 nm	1400 °C, 2 h	$\sigma_{600\ °C} = 10^{-4}$ S cm^{-1}	47
$Ce_{0.9}Gd_{0.1}O_{1.95}$	MW assisted polyol method	3.6 nm	170 °C, 2 h	–	48
$La_{9.33}Si_2Ge_4O_{26}$	MW assisted mechanical alloying	1.1 μm	1350 °C, 1 h	–	53
$Ce_{0.8}Sm_{0.18}Ca_{0.02}O_{1.9}$	MW assisted hydrothermal method	2 μm	1450 °C, 5 min	–	54
$LiCe_{0.9}Gd_{0.1}O_{2-\delta}$	MW sintering with lithium nitrate aid	150 nm	600 °C, 1 h	$\sigma_{600\ °C} = 10^{-2}$ S cm^{-1}	55
$Sm_{0.2}Ce_{0.8}O_{2-\delta}$	MW assisted combustion method	300–800 nm	1200 °C	0.86 W cm^{-2} (650 °C)	72
10Sc1CeSZ	MW assisted glycine nitrate process	19.2 nm	900 W	$\sigma_{800\ °C} = 1.84 \times 10^{-1}$ S cm^{-1}	57
$Ce_{0.85}La_{0.075}Sm_{0.075}O_{2-\delta}$	MW assisted hydrothermal method	50 nm	1200 °C, 30 min	$\sigma_{600\ °C} = 2.10 \times 10^{-2}$ S cm^{-1}	63
$Ce_{0.8}Pr_{0.2-x}Dy_xO_{2-\delta}$	MW assisted sol-gel method	225 nm	1300 °C, 30 min	$\sigma_{500\ °C} = 6.8 \times 10^{-3}$ S cm^{-1}	64
$Ce_{0.76}Pr_{0.08}Sm_{0.08}Gd_{0.08}O_{2-\delta}$	MW assisted sol-gel method	229 nm	1300 °C, 30 min	$\sigma_{600\ °C} = 3.47 \times 10^{-2}$ S cm^{-1}	66
$Ce_{0.8}Sm_{0.2-x}Y_xO_{2-\delta}$	MW assisted sol-gel method	293–465 nm	1200 °C, 1 h	$\sigma_{600\ °C} = 2.50 \times 10^{-2}$ S cm^{-1}	65
$BaZr_{0.1}Ce_{0.66}Ni_{0.04}Y_{0.2}O_{3-\delta}$	MW assisted anode-electrolyte co-sintering process	–	1100 °C, 2 h	0.49 W cm^{-2} (700 °C)	67
$BaCe_{0.7}Zr_{0.1}Y_{0.2}O_{3-\delta}$	MW assisted anode-electrolyte co-sintering process	600 nm	1200 °C, 2 h	$\sigma_{700\ °C} = 1.4 \times 10^{-2}$ S cm^{-1}	68
$BaZr_{0.1}Ce_{0.7}Y_{0.2}O_{3-\delta}$	MW assisted anode-electrolyte co-sintering process	–	1200 °C, 2 h	–	73

Note. δ is non-stoichiometric oxides, σ is electrical conductivity.

Table 2. Brief summary of microwave assisted preparation of anode materials.

Anode powders	Fabrication process	Grain size	Microwave processing	Ref.
NiO/YSZ	MW assisted combustion method	~15 nm	10 s (1200 W, 2.45 GHz)	74
Cu–Ni/YSZ	MW assisted adhesion of Cu particles on Ni/YSZ	~21 nm	60 s (700 W, 2.45 GHz)	80
Ni/YSZ	MW assisted anode-electrolyte co-sintering	–	1600 °C, 8 min	45
$La_{0.3}Sr_{0.7}Ti_{0.9}Nb_{0.1}O_3$	MW assisted combustion	–	300 W, 3 min (5% H_2+95% Ar)	81
$NiOCe_{1-x}Eu_xO_{2-\delta}$	MW assisted hydrothermal synthesis	–	900 °C, 1 h	82
YSZ-CeO_2	MW assisted hydrothermal synthesis	14 nm	130 °C, 2 h; 1200 °C, 3 h	83
$NiOCe_{0.5}Zr_{0.5}O_2$	MW assisted combustion method	14 nm	700 °C, 2 h	75
NiO–YSZ–CeO_2	MW assisted hydrothermal synthesis	750 nm	130 °C, 2 h; 500 °C, 4 h	78
NiO–ZrO_2–Y_2O_3–TiO_2	MW assisted mechanical mixed oxide method	–	1400 °C, 30 min (900 W, 2.45 GHz)	84
NiO/10Sc1CeSZ	MW assisted glycine nitrate combustion	30–60 nm	3 s (700 W, 2.5 GHz)	76
Manganese anode mud	MW assisted solid phase reaction	–	10 min (1000 W, 2.45 GHz)	85
NiO/SDC	MW assisted glycine nitrate combustion	7 nm	133W–532W–798W in an on/off cycle (10 s on and 20 s off) for 10 min	86

Note. δ is non-stoichiometric oxides.

there are two main types of SOFC anode materials: metal-based anodes and chalcogenide-based anodes, there are also other types of anodes. Among these, nickel-based anodes have the highest catalytic activity and are relatively inexpensive, making them popular among researchers. However, nickel-based anodes tend to self-sinterer, which reduces porosity and results in a smaller three-phase interface area. This in turn negatively affects the electrochemical performance of the anode. To overcome these limitations, composite anodes have been developed that combine conductive materials such as nickel oxide (NiO) with ion-conductive materials, yttria-stabilized zirconia (YSZ), and gadolinium-doped ceria (GDC) have been developed.

Because of its advantages in terms of rapid heating, microwave sintering technology is also being considered for the preparation of anodes for solid oxide fuel cells. Remarkably, numerous studies have shown that microwave sintering technology has unique advantages in the regulating of the crystal phase structure, which significantly affects the catalytic activity of the anode. The microwave assisted synthesis of nanocomposite powders, uses water-soluble nitrates, citric acid, and ethylene glycol as starting materials. This particular technique facilitates the synthesis of uniform nanocomposite powders, such as NiO–YSZ, NiO–$Ce_{0.5}Zr_{0.5}O_2$, and Ni–10Sc1CeZr.[74–76] In addition, microwave assisted hydrothermal synthesis has been used to synthesize NiO–$Ce_{1-x}Eu_xO_{2-\delta}$ powders, which can be used to replace conventional NiO–YSZ anodes in SOFCs.[77] The use of microwave assisted hydrothermal synthesis facilitates the formation of crystalline β-nickel hydroxide at low temperatures, resulting in larger grain sizes of NiO in NiO–YSZ–CeO_2 composites.[78] Nanoscale anode powders can increase the area of the triple-phase boundary (TPB), resulting in a lower activation energy for oxygen ion conduction, thus improving anode performance. Rapid microwave irradiation is also a technology that can be used to prepare carbon-tolerant anode in a short period of time.[79,80] In addition, microwave sintering is used to anode-electrolyte co-sintering due to its ability to produce high-density electrolytes rapidly and easily.[45] Furthermore, the rapid microwave sintering method allows the creation of pure perovskite phase structures in a reducing atmosphere. The conductivity of $La_{0.3}Sr_{0.7}Ti_{0.9}Nb_{0.1}O_3$ (LSTN) prepared under a 5% H_2+95% Ar atmosphere in the microwave cavity was higher than that of conventional sintering, because the reducing atmosphere increased the reduction conversion of Ti^{4+} to Ti^{3+}, which contributed to the higher oxygen ion conductivity.[81]

In summary, microwave sintering technology can assist in the rapid synthesis of nanoscale anode powders with increased specific surface area, which serves as the site for the catalytic fuel oxidation reaction. Table 2 provides a summary of the investigations on the application of microwave heating technology to anode materials, including the specific methods used and the corresponding synthesis times and powder grain sizes obtained. The table provides an overview of the various microwave-assisted powder synthesis techniques documented in the scientific literature, including microwave hydrothermal synthesis, microwave assisted combustion, and microwave-assisted sol-gel processes.

3.3. Cathode materials

The solid oxide fuel cell cathode, also known as the oxygen electrode, is the site of reactions, such as oxygen adsorption, dissociation, and diffusion. The key characteristics of ideal SOFC cathode materials are as following: high catalytic activity for oxygen reduction reactions, high electron conductivity, and ionic conductivity, suitable porosity and large specific surface area, high chemical stability in an oxidizing atmosphere, reasonable chemical compatibility and a thermal expansion coefficient similar to that of the electrolytes.

The cathodes are usually prepared by screen printing, spin coating, impregnation-coating, flow retardation, etc. The void ratio and pore size of the cathodes are controlled by adjusting the type and amount of pore-forming agent and the sintering process of the cathodes. However, in order to achieve good adhesion between the cathode and electrolyte, the sintering temperature of the cathode usually reaches 1000–1200 °C. At such high sintering temperatures, the cathode particles grow rapidly, usually to the micron level. As the particle size increases, the specific surface area of the cathode decreases, resulting in less contact area with the air which is closely related to the TPB and the reactive capacity of the cathode.

Due to their small particle size, large specific surface area, and high catalytic activity, nanocathodes have become a hot topic of research in medium temperature SOFC research in recent years. As the particle size decreases, the specific surface area of the material increases, allowing for a larger three-phase reaction interface and more active sites for oxygen reduction, which can significantly reduce the polarization resistance of the cathode. A microwave-assisted pore wetting technique was used to prepare nanotube structure of $La_{0.6}Sr_{0.4}Co_{0.2}Fe_{0.8}O_3$, which

exhibits excellent cathode performance for SOFCs.[87] Compared with conventional micro-structured materials, the surface of the nanotubue cathode prepared using microwave irradiation technology has more active reaction sites. Microwave assisted combustion technology has also been used to prepare mixed ion-electron conducting nanoscale cathode materials. Nanoscale $Nd_{1.8}Ce_{0.2}Cu_{0.5}Ni_{0.5}O_{4+\delta}$ cathode powders produced by microwave-assisted combustion are considered a potential cathode material for SOFC applications due to their good electrocatalytic activity for oxygen reduction.[88] Since a material itself converts microwave energy into heat *via* electromagnetic field coupling, the gel can quickly reach its autoignition temperature. The resulting precursor powders can be sintered at high temperatures to achieve effective powder microstructure control.[89–91] Other mixed ionic electronic conductors (MIECs) of the A_2BO_4 (A is rare earth element, alkaline earth metal; B is transition metal) type structure, such as $Nd_{1.8}Sr_{0.2}NiO_{4+\delta}$ (Ref. 92) and $Pr_{1.6}Sr_{0.4}CuO_{4\pm\delta}$ (Ref. 93), have attracted the attention to microwave technology because of their high electronic conductivity, sufficient oxygen ion conductivity and strong electrocatalytic activity towards oxygen reduction reaction (ORR).

In addition, some ABO_3-structured perovskite cathode materials with mixed electronic and ionic conductivity, such as $La_{0.6}Sr_{0.4}Co_{0.2}Fe_{0.8}O_{3-\delta}$(LSCF), are chemically compatible with barium cerate-based electrolyte materials.[94] Ali *et al.*[95] investigated the effect of microwave energy on the properties of LSCF powders synthesized by the microwave-assisted combustion method. Figure 10 shows the microstructures of LSCF synthesized by microwave combustion and conventional combustion. The cross-sectional views of the conventional-LSCF and microwave-LSCF films deposited on the electrolyte surface are shown in Fig. 10*a*,*b*, respectively. Microwave LSCF films are more porous (Fig. 10*d*) than conventional LSCF films (Fig. 10*c*). Fig. 10*d* also shows continuous voids, which can facilitate the migration of oxygen ions. A porosity of 30% to 40% allows for easy oxygen transport through the porous body of the microwave LSCF cathode, occupying the adsorption sites on LSCF and enhancing electron transfer. Microwave LSCF had small particle sizes and uniformly distributed pores, resulting in a highly porous structure (Fig. 10*b*,*d*). This result can be attributed to the different powder morphologies, calcination temperatures, and solid contents of LSCF.As a result, microwave heating can be used to prepare LSCF powders and create an optimal porous structure. Furthermore, the performance of microwave combustion cathode is superior to that of conventional heating cathode. The investigation of $La_{0.7-x}Pr_xCa_{0.3}MnO_3$ prepared by microwave-assisted combustion showed that the synthesis method of microwave assisted combustion can modulate the microscopic morphology of powders and promote the conductivities.[96] A pure perovskite $La_{0.7}Sr_{0.3}Fe_{0.7}Ga_{0.3}O_{3-\delta}$ was prepared in the air by the microwave assisted combustion method and evaluated as an electrode for a symmetrical solid oxide fuel cell.[97]

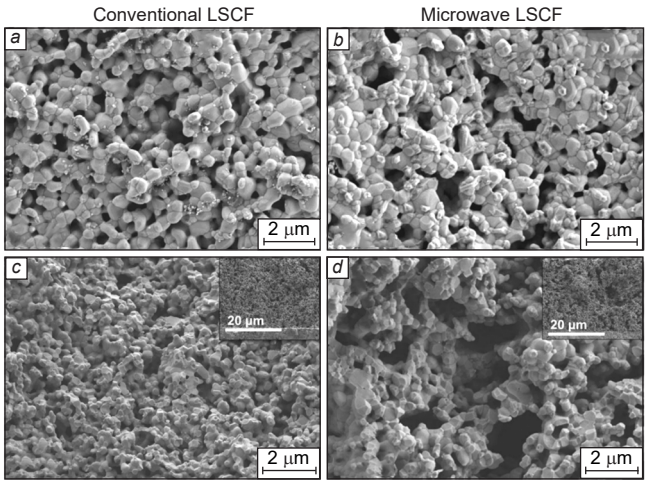

Figure 10. SEM images of surfaces (*a*, *b*) and cross sections (*c*, *d*) of pellets sintered at 1200 °C: (*a*, *c*) conventional LSCF and (*b*, *d*) microwave LSCF. (Reprinted with permission from Ref. 95. Copyright 2017 Elsevier.)

Some studies have found that microwave heating can promote the rapid adhesion of the cathode layer to the electrolyte layer and reduce not only the sintering temperature but also the

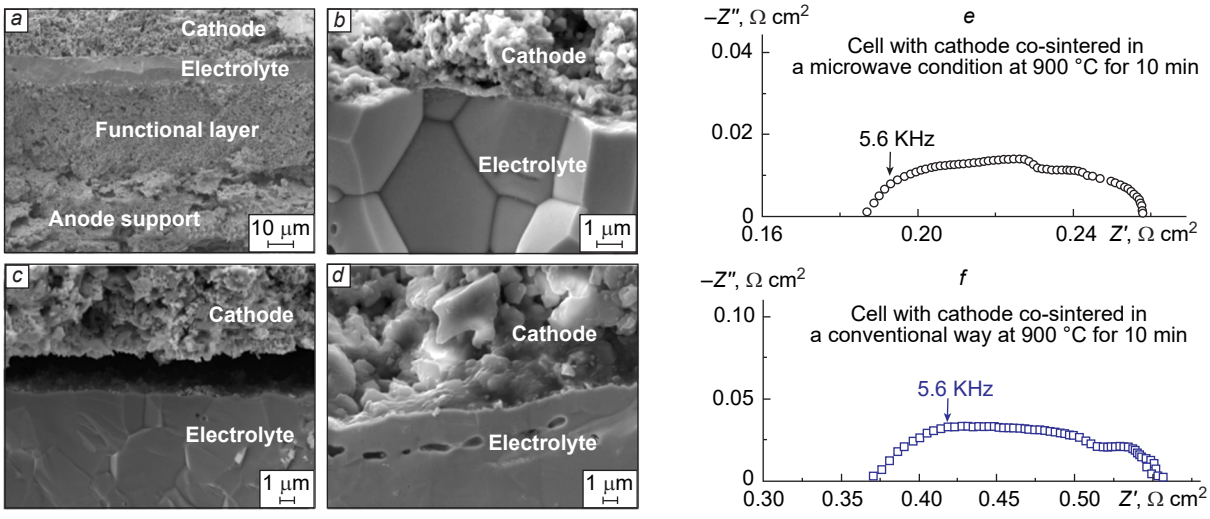

Figure 11. SEM images for (*a*) the section of a fabricated cell, (*b*) cathode/electrolyte interface (microwave-assisted cathode co-sintered at 900 °C for 10 min); (*c*) cathode/electrolyte interface (conventional method assisted cathode co-sintered at 900 °C for 10 min) and (*d*) cathode/electrolyte interface (conventional method assisted cathode co-sintered at 1000 °C for 2 h); electrochemical impedance spectra of the cells with a $Ba_{0.5}Sr_{0.5}Co_{0.8}Fe_{0.2}O_{3-\delta}$ (BSCF) cathode co-sintered at 900 °C for 10 min by (*e*) microwave sintering, (*f*) conventional sintering. (Reprinted with permission from Ref. 98. Copyright 2019 Elsevier.)

Table 3. A brief summary of microwave assisted preparation of cathode materials.

Cathode powders	Fabrication process	Grain size	Microwave processing	Electrochemical properties	Ref.
$Ln_{0.7}Sr_{0.3-x}Ca_xCO_{0.9}Fe_{0.1}O_{3-\delta}$ (x = 0.05, 0.10, 0.15)	MW assisted solid phase synthesis	1–20 μm	1200 °C, 30 min	$\sigma_{700\ °C}$ = 100 S cm^{-1}	101
$La_{0.6}Sr_{0.4}Co_{0.2}Fe_{0.8}O_3$ nanotubes	MW assisted pore wetting	20 nm	6 min	–	87
$La_{0.1}Sr_{0.9}Co_{0.8}Fe_{0.2}O_{3-\delta}$	MW assisted cathode layer screen printing	–	950 °C, 2 min	Cathode ASR (650 °C) = 0.014 Ω cm^2	102
$Nd_{1.8}Ce_{0.2}Cu_{0.5}Ni_{0.5}O_{4+\delta}$	MW assisted sol-gel combustion	185 nm	800 W	$\sigma_{700\ °C}$ = 0.619 S cm^{-1}	88
$Nd_{1.8}Sr_{0.2}NiO_{4+\delta}$	MW assisted sol-gel combustion	166 nm	1200 °C, 4 h	$\sigma_{660\ °C}$ = 61 S cm^{-1}	92
$La_{0.6}Sr_{0.4}Co_{0.2}Fe_{0.8}O_{3-\delta}$–20 wt.% $Ce_{0.78}Gd_{0.2}Sr_{0.02}O_{2-\delta}$	MW assisted cathode layer screen printing	–	1000 °C, 1 h	$R_{P\ 700\ °C}$= 6.6 Ω cm^2	103
$La_{1.7}Sm_{0.3}Mo_2O_9$	MW assisted combustion	25 nm	900 W, 10 min	$\sigma_{750\ °C}$ = 0.196 S cm^{-1}	104
$La_{0.7}Sr_{0.3}Fe_{0.7}Ga_{0.3}O_{3-\delta}$	MW assisted combustion	26.8–35.1 nm	–	$\sigma_{800\ °C}$ = 47.45 S cm^{-1}	97
$La_{0.6}Sr_{0.4}Co_{0.2}Fe_{0.8}O_{3-\delta}$	MW assisted combustion	113 nm	650–700 W, 10 min	Cathode ASR (750 °C) = 0.097 Ω cm^2	95
$Sm_{0.5}Sr_{0.5}CoO_{3-\delta}$–$BaZr_{0.1}Ce_{0.7}Y_{0.2}O_{3-\delta}$	MW assisted electrolyte-cathode co-sintering	–	1100 °C, 2 h	MPD $_{700\ °C}$ = 449 mW cm^{-2}	67
$Pr_{1.6}Sr_{0.4}CuO_{4\pm\delta}$	MW assisted combustion	728 nm	1000 °C, 4 h	$\sigma_{700\ °C}$ = 63.1 S cm^{-1}	93
$Ba_{0.5}Sr_{0.5}Co_{0.8}Fe_{0.2}O_{3-\delta}$	MW assisted cathode layer deposition	–	900 °C, 10 min	MPD $_{700\ °C}$ = 0.96 mW cm^{-2}	98
$La_{0.6}Sr_{0.4}Co_{0.2}Fe_{0.8}O_{3-\delta}$–$Ce_{0.8}Sm_{0.2}O_{1.9}$	MW assisted combustion	79–96 nm	900 W, 5 min	$R_{P\ 700\ °C}$ = 0.68 Ω cm^2	105
$La_{0.07}Pr_{0.63}Ca_{0.3}MnO_3$	MW assisted combustion	–	900 W, 4 min	$\sigma_{700\ °C}$ = 0.68 S cm^{-1}	96
$La_{0.6}Ca_{0.4}Ni_{0.2}Fe_{0.8}O_3$	MW assisted combustion	–	–	$\sigma_{700\ °C}$ = 29.6 S cm^{-1}	106

Note. δ is non-stoichiometric oxides, σ is electrical conductivity, R_P is polarization resistance, MPD is maximum power density, ASR is area specific resistance.

sintering time. Bi and coworkers took the lead in studying the application of microwave sintering technology to proton-conducting SOFCs(H-SOFCs), exploring the effect of microwave fields on cathode morphology, electrolyte-cathode layer interface and electrochemical performance.[28,98] Figures 11 *b–d* show the SEM images of cathode electrolyte interfaces after fuel cell testing. Cathodes sintered at 900 °C for 10 min by microwave and conventional technologies were both porous, while the microwave sintered cathode layer adhered better to the electrolyte than the conventional sintering one. Although good cathode-electrolyte adhesion can be achieved by conventional sintering, increasing the cosintering temperature and calcination time increases the cathode grain size while decreasing the porosity.[99,100] Electrochemical impedance spectroscopy confirmed that low cathode porosity increases polarization resistance and poor cathode-electrolyte adhesion increases ohmic resistance Fig. 11 *e–f*.

In general, microwave sintering technology is widely used in the cathode treatment of solid oxide fuel cells. The latest research results on cathode treatment using microwave technology are collected and shown in Table 3. Microwave technology can not only control the microscopic phase properties of the cathode, such as porosity and TPB, but also improve the adhesion of the cathode-electrolyte layer and reduce the interfacial resistance.

4. Conclusion and perspective

In this review, we have witnessed the application of microwave technology to SOFC production over the past decade. Microwave sintering technology, unlike traditional sintering methods, converts electromagnetic energy into thermal energy due to the dielectric losses of the material when exposed to electromagnetic waves. Due to its unique heating mechanism, microwave sintering technology has the advantage of low temperature and period in the synthesis of materials, and the material microstructure can be well regulated.

As this review has shown, microwave heating technology can be used to optimize the microstructure of the electrolyte, anode, and cathode, the three main components of fuel cells. By applying microwave energy, it is possible to increase the density of the electrolyte and decrease the resistance of the material in bulk and grain boundary. For the anode, microwave treatment can effectively control the microstructure to increase the catalytic activity. For the cathode, microwave treatment can also optimize the interface with the electrolyte as well as improve the microstructure and enhance the catalytic activity.

Although great progress has been made in recent years in solid oxide fuel cells using microwave treatment technology, several key issues remain to be addressed to propose future research directions.

(1) *Further fundamental study of the influence of electromagnetic waves on the properties of SOFC materials*. The dielectric losses of a material correlate with the efficiency of its absorption of electromagnetic waves, which in turn closely relates to the efficiency of sintering. The study of electromagnetic-thermal stress fields will improve the sintering efficiency, leading to the optimization of the cathode-electrolyte interface and, consequently, to improved electrochemical performance.

(2) *In-depth study of the influence of microwave treatment on microscopic morphology of SOFC materials*. The regulation of the microscopic morphology of materials by microwave heating is currently limited to the regulation of crystal size, but only further studies will show the influence on grain boundary growth, defect generation and conductivity variation.

5. List of acronyms and designations

BZCY — $BaCe_{0.7}Zr_{0.1}Y_{0.2}O_{3-\delta}$,
CMC — ceramic matrix composite,

GDC — $Ce_{0.9}Gd_{0.1}O_{1.95}$,
H-SOFC — proton conducting solid oxide fuel cells,
LSCF — $La_{0.6}Sr_{0.4}Co_{0.2}Fe_{0.8}O_{3-\delta}$,
LSGM — $La_{0.8}Sr_{0.2}Ga_{0.83}Mg_{0.17}O_{2.815}$,
MIEC — mixed ionic-electronic conductor,
OCV — open circuit voltage,
SDC — $Ce_{0.8}Sm_{0.2}O_{19}$,
SOFC — solid oxide fuel cells,
TPB — triple-phase boundary,
YSZ — yttria-stabilized zirconia.

6. References

1. F.Zhang, K.S.Gallagher, Z.Myslikova, E.Narassimhan, R.R.Bhandary, P.Huang. *Wiley Interdisciplinary Reviews-Climate Change*, **12**, 734 (2021); https://doi.org/10.1002/wcc.734
2. J.D.Chen, M.Gao, M.Shahbaz, S.L.Cheng, M.L.Song. *Renewable and Sustainable Energy Reviews*, **145**, 111141 (2021); https://doi.org/10.1016/j.rser.2021.111141
3. Y.J.Wang, J.B.Huang. *Energy*, **261** (2022); https://doi.org/10.1016/j.energy.2022.124964
4. A.Aslan, O.Ocal, B.Ozsolak, I.Ozturk. *Renewable Energy*, **188**, 402 (2022); https://doi.org/10.1016/j.renene.2022.02.039
5. J.Q.Huang, Z.X.Yu, J.L.Tang, P.Q.Wang, Q.Y.Tan, J.Wang, X.Z.Lei. *Int. J. Hydrogen Energy*, **47**, 27800 (2022); https://doi.org/10.1016/j.ijhydene.2022.06.140
6. A.B.Stambouli, E.Traversa. *Renewable and Sustainable Energy Reviews*, **6**, 433 (2002); https://doi.org/10.1016/S1364-0321(02)00014-X
7. Y.Gao, M.Zhang, M.Fu, W.Hu, H.Tong, Z.Tao. *Energy Rev.*, 100038 (2023); https://doi.org/10.1016/j.enrev.2023.100038
8. F.Ramadhani, M.A.Hussain, H.Mokhlis, S.Hajimolana. *Renewable and Sustainable Energy Reviews*, **76**, 460 (2017); https://doi.org/10.1016/j.rser.2017.03.052
9. H.Tong, M.Fu, Y.Yang, F.Chen, Z.Tao. *Adv. Functional Mater.*, **32**, 48 (2022); https://doi.org/10.1002/adfm.202209695
10. S.G.Chen, H.X.Zhang, C.A.Yao, H.Lou, M.C.Chen, X.S.Lang, K.D.Cai. *Energy Fuels*, 48 (2023); https://doi.org/10.1021/acs.energyfuels.2c03934
11. A.R.Noviyanti, Juliandri, S.Winarsih, D.G.Syarif, Y.T.Malik, R.Septawendar, Risdiana. *RSC Adv.*, **11**, 61 (2021); https://doi.org/10.1039/D1RA07223D
12. B.Steele. *Solid State Ionics*, **134**, 3 (2000); https://doi.org/10.1016/S0167-2738(00)00709-8
13. V.Palma, D.Barba, M.Cortese, M.Martino, S.Renda, E.Meloni. *Catalysts*, **10** (2020); https://doi.org/10.3390/catal10060665
14. R.Wei, P.Wang, G.S.Zhang, N.N.Wang, T.Zheng. *Chem. Eng. J.*, **382** (2020); https://doi.org/10.1016/j.renene.2022.02.039
15. Z.Wang, C.Yu, H.W.Huang, W.Guo, J.H.Yu, J.S.Qiu. *Nano Energy*, **85** (2021); https://doi.org/10.1016/j.nanoen.2021.105942
16. Y.F.Sun, P.Zhang, J.P.Hu, B.C.Liu, J.K.Yang, S.Liang, K.K.Xiao, H.J.Hou. *Construc. Build. Mater.*, **294** (2021); https://doi.org/10.1016/j.conbuildmat.2021.123476
17. S.Alem, R.Latifi, S.Angizi, F.Hassanaghaei, M.Aghaahmadi, E.Ghasali, M.Rajabi. *Mater. Manufact. Proc.*, **35**, 3 (2020); https://doi.org/10.1080/10426914.2020.1718698
18. D.V.Dudina, K.Georgarakis, E.A.Olevsky. *Int. Mater. Rev.*, **68**, 2 (2023); https://doi.org/10.1080/14432471.2023.2236756
19. Y.J.Kim, B.H.Ryu, H.Jin, J.Lee, H.S.Shin. *Ceramics Int.*, **47**, 19 (2021); https://doi.org/10.1016/j.ceramint.2021.06.098
20. X.Wang, Z.Liu, Y.Tang, J.Chen, D.Wang, Z.Mao. *J. Power Sources*, **481** (2021); https://doi.org/10.1016/j.jpowsour.2020.228824
21. X.Zhang, J.Wang, J.Wen, Y.Wang, N.Li, J.Wang, L.Fan. *Ceramics Int.*, **48**, 13 (2022); https://doi.org/10.1016/j.ceramint.2022.03.185
22. S.Egorov, A.Eremeev, V.Kholoptsev, I.Plotnikov, K.Rybakov, A.Sorokin, S.Balabanov, E.Y.Rostokina. *Ceramics Int.*, **49**, 14 (2023); https://doi.org/10.1016/j.ceramint.2022.11.203
23. T.G.Evangeline, A.R.Annamalai. *Ceramics Int.*, **48**, 18 (2022); https://doi.org/10.1016/j.ceramint.2022.05.179
24. K.W.Yeung, C.Y.Tang, R.Hu, C.H.Lam, W.C.Law, G.C.P.Tsui, X.Zhao, J.K.H.Chung. *J. Eur. Ceramic Society*, **42**, 10 (2022); https://doi.org/10.1016/j.jeurceramsoc.2022.03.046
25. N.Khalile, C.Petit, C.Meunier, F.Valdivieso. *Ceramics Int.*, **48**, 13 (2022); https://doi.org/10.1016/j.ceramint.2022.03.072
26. G.Evangeline T, R.Annamalai A, P.Ctibor. *Molecules*, **28**, 4 (2023); https://doi.org/10.3390/molecules28041649
27. A.Hussain, M.ul Hassan, R.H.Song, M.Z.Khan, A.M.Mehdi, H.J.Ryu, T.H.Kim, J.E.Hong, D.W.Joh, S.B.Lee. *Ceramics Int.*, **49**, 18 (2023); https://doi.org/10.1016/j.ceramint.2023.06.309
28. S.Yu, Y.Gu, L.Bi. *Russ. Chem. Rev.*, **91** (11), RCR5061 (2022); https://doi.org/10.57634/RCR5061
29. D.A.Jones, T.Lelyveld, S.Mavrofidis, S.Kingman, N.Miles. *Resources, Conservation and Recycling*, **34**, 2 (2002); https://doi.org/10.1016/S0921-3449(01)00088-X
30. R.E.Collin. *Foundations for Microwave Engineering*. (John Wiley & Sons, 2007)
31. G.H.Owyang. *Foundations for Microwave Circuits*. (Springer Science & Business Media, 2012)
32. C.Saltiel, A.K.Datta. In *Advances in Heat Transfer*. Vol. 33. (Elsevier, 1999). P. 1
33. Z.Fu, A.Pang, H.Luo, K.Zhou, H.Yang. *J. Mater. Res. Technol.*, **18** (2022); https://doi.org/10.1016/j.jmrt.2022.03.164
34. J.Samuels, J.Brandon. *J. Mater. Sci.*, **27**, 3259 (1992); https://doi.org/10.1007/BF01116022
35. D.Ding. *Adv. Ceramic Matrix Composites*, 9 (2014); https://doi.org/10.1016/B978-0-08-102166-8.00002-5
36. R.R.Mishra, A.K.Sharma. *Composites, Part A: Appl. Sci. Manufacturing*, **81**, 78 (2016); https://doi.org/10.1016/j.compositesa.2015.10.035
37. R.Subasri, T.Mathews, O.Sreedharan. *Mater. Lett.*, **57**, 1792 (2003); https://doi.org/10.1016/S0167-577X(02)01070-4
38. B.Rambabu, S.Ghosh, W.Zhao, H.Jena. *J. Power Sources*, **159**, 21 (2006); https://doi.org/10.1016/j.jpowsour.2006.04.107
39. Y.L.Zhai, C.Ye, F.Xia, J.Z.Xiao, L.Dai, Y.F.Yang, Y.Q.Wang. *J. Power Sources*, **162**, 1 (2006); https://doi.org/10.1016/j.jpowsour.2006.06.069
40. B.Rambabu, S.Ghosh, H.Jena. *J. Mater. Sci.*, **41**, 7530 (2006); https://doi.org/10.54302/mausam.v57i1.463
41. R.Chockalingam, V.R.W.Amarakoon, H.Giesche. *J. Eur. Ceramic Society*, **28**, 959 (2008); https://doi.org/10.1016/j.jeurceramsoc.2007.09.031
42. X.T.Wang, G.M.Kale. *Key Eng. Mater.*, **268**–**372** (2008); https://doi.org/10.4028/www.scientific.net/KEM.368-372.238
43. Z.Jiao, N.Shikazono, N.Kasagi. *J. Power Sources*, **195**, 151 (2010); https://doi.org/10.1016/j.jpowsour.2009.07.009
44. H.Y.Chang, Y.M.Wang, C.H.Lin, S.Y.Cheng. *J. Power Sources*, **196**, 1704 (2011); https://doi.org/10.1016/j.jpowsour.2010.10.035
45. Z.Jiao, N.Shikazono, N.Kasagi. *J. Power Sources*, **196**, 13 (2011); https://doi.org/10.1016/j.jpowsour.2011.02.040
46. S.A.Acharya. *J. Power Sources*, **198**, 15 (2012); https://doi.org/10.1016/j.jpowsour.2011.09.087
47. Y.f.Bu, Q.Zhong, W.y.Tan, R.j.Zhou, Y.Song, W.Cai. *Mater. Sci. Semiconduc. Proc.*, **16**, 6 (2013); https://doi.org/10.1016/j.mssp.2013.07.034
48. A.Gondolini, E.Mercadelli, A.Sanson, S.Albonetti, L.Doubova, S.Boldrini. *J. Eur. Ceramic Society*, **33**, 1 (2013); https://doi.org/10.1016/j.jeurceramsoc.2012.08.008
49. D.Han, J.Iihara, S.Uemura, K.Kazumi, C.Hiraiwa, M.Majima, T.Uda. *J. Mater. Chem., A*, **4**, 10601 (2016); https://doi.org/10.1039/C6TA03552C
50. H.Zhang, B.A.Wilhite. *J. Membrane Sci.*, **512**, 15 (2016); https://doi.org/10.1016/j.memsci.2016.04.001
51. C.Yang, H.Zhao, Z.Du, Y.Shen, C.Yan. *J. Membrane Sci.*, **508**, 104 (2016); https://doi.org/10.1016/j.memsci.2016.02.032

52. L.Yang, C.Zuo, S.Wang, Z.Cheng, M.Liu. *Adv. Mater.*, **20**, 17 (2008); https://doi.org/10.1002/adma.200702762
53. M.Santos, C.Alves, F.A.C.Oliveira, T.Marcelo, J.Mascarenhas, A.Cavaleiro, B.Trindade. *J. Power Sources*, **231**, 146 (2013); https://doi.org/10.1016/j.jpowsour.2012.12.101
54. J.Prado-Gonjal, R.Heuguet, D.Munoz-Gil, A.Rivera-Calzada, S.Marinel, E.Moran, R.Schmidt. *Int. J. Hydrogen Energy*, **40**, 45 (2015); https://doi.org/10.1016/j.ijhydene.2015.07.161
55. H.P.Dasari, K.Ahn, S.Y.Park, J.Hong, H.Kim, K.J.Yoon, J.W.Son, B.K.Kim, H.W.Lee, J.H.Lee. *J. Alloys Compd.*, **672**, 397 (2016); https://doi.org/10.1016/j.jallcom.2016.02.184
56. S.S.B.C.Abdullah, T.Teranishi, H.Hayashi, A.Kishimoto. *Mater. Design*, **115**, 231 (2017); https://doi.org/10.1016/j.matdes.2016.11.051
57. A.A.Jais, S.A.M.Ali, M.Anwar, M.R.Somalu, A.Muchtar, W.N.R.W.Isahak, C.Y.Tan, R.Singh, N.P.Brandon. *Ceramics Int.*, **43**, 11 (2017); https://doi.org/10.1016/j.ceramint.2017.03.135
58. W.Sun, W.Liu. *J. Power Sources*, **217**, 114 (2012); https://doi.org/10.1016/j.jpowsour.2012.05.065
59. S.Jadhav, V.Puri, L.Jadhav. *J. Alloys Compd.*, **685**, 626 (2016); https://doi.org/10.1016/j.jallcom.2016.05.243
60. A.Jacobson, B.t. Tofield, B.Fender. *Acta Crystallogr. Section B: Struct. Crystallog. Crystal Chem.*, **28**, 956 (1972); https://doi.org/10.1107/S0567740872003462
61. S.Dubal, A.Jamale, S.Jadhav, S.Patil, C.Bhosale, L.Jadhav. *J. Alloys Compd.*, **587**, 664 (2014); https://doi.org/10.1016/j.jallcom.2013.10.093
62. A.S.Kumar, R.Balaji, S.Jayakumar. *Mater. Chem. Phys.*, **202**, 82 (2017); https://doi.org/10.1016/j.matchemphys.2017.09.008
63. M.Gupta, S.Shirbhate, P.Ojha, S.Acharya. *Solid State Ionics*, **320**, 199 (2018); https://doi.org/10.1016/j.ssi.2018.03.005
64. C.Madhusudan, K.Venkataramana, C.Madhuri, C.V.Reddy. *J. Mater. Sci.-Mater. Electron.*, **29**, 17067 (2018); https://doi.org/10.1007/s10854-018-9803-8
65. K.Venkataramana, K.Ravindranath, C.Madhuri, C.Madhusudan, N.Pavan Kumar, C.Vishnuvardhan Reddy. *Ionics*, **24**, 1429 (2018); https://doi.org/10.1007/s11581-017-2293-5
66. K.Venkataramana, C.Madhuri, J.Shanker, C.Madhusudan, C.V.Reddy. *Ionics*, **24**, 3075 (2018)
67. B.Wang, L.Bi, X.S.Zhao. *J. Eur. Ceramic Society*, **38**, 16 (2018); https://doi.org/10.1016/j.jeurceramsoc.2018.08.020
68. X.Xu, L.Bi, X.S.Zhao. *J. Membr. Sci.*, **558**, 17 (2018); https://doi.org/10.1016/j.memsci.2018.04.037
69. D.Han, Y.Otani, Y.Noda, T.Onishi, M.Majima, T.Uda. *RSC Adv.*, **6**, 19288 (2016); https://doi.org/10.1039/C5RA26947D
70. A.Gondolini, E.Mercadelli, A.Sanson, S.Albonetti, L.Doubova, S.Boldrini. *Ceramics Int.*, **37**, 4 (2011); https://doi.org/10.1016/j.ceramint.2011.01.010
71. C.Alves, T.Marcelo, F.A.C.Oliveira, L.C.Alves, J.Mascarenhas, B.Trindade. *J. Eur. Ceramic Society*, **33**, 12 (2013); https://doi.org/10.1016/j.jeurceramsoc.2012.12.024
72. H.Sun, Y.Zhang, H.Gong, Q.Li, Y.Bu, T.Li. *Ceramics Int.*, **42**, 3 (2016); https://doi.org/10.1016/j.ceramint.2015.11.105
73. B.Wang, X.Liu, L.Bi, X.Zhao. *J. Power Sources*, **412**, 664 (2019); https://doi.org/10.1016/j.jpowsour.2018.11.051
74. C.Tongxiang, Z.Yanwei, Z.Wei, G.Cuijing, Y.Xiaowei. *J. Power Sources*, **195**, 5 (2010); https://doi.org/10.1016/j.jpowsour.2009.09.027
75. J.Feng, J.Qiao, W.Sun, P.Yang, H.Li, Z.Wang, K.Sun. *Int. J. Hydrogen Energy*, **40**, 37 (2015); https://doi.org/10.1016/j.ijhydene.2015.07.121
76. A.A.Jais, S.Ali, M.Anwar, M.R.Somalu, A.Muchtar, W.N.R.W.Isahak, N.A.Baharudin, K.L.Lim, N.P.Brandon. *J. Solid State Electrochem.*, **24**, 711 (2020); https://doi.org/10.1007/s10008-020-04512-6
77. A.L.de Medeiros, A.E.Martinelli, D.M.de Araujo Melo, M.O.Orlandi, D.A.Macedo. *Electrochem. Society*, **44** (2014); https://doi.org/10.1149/06136.0001ecst
78. L.Pinheiro, F.Tabuti, A.Martinelli, F.Fonseca. *Ceramics Int.*, **42**, 7 (2016); https://doi.org/10.1016/j.ceramint.2016.02.165
79. S.Islam, J.M.Hill. *ECS Transactions*, **35**, 1389 (2011); https://doi.org/10.1149/1.3570125
80. S.Islam, J.M.Hill. *J. Power Sources*, **196**, 11 (2011); https://doi.org/10.1016/j.jpowsour.2011.01.087
81. H.Y.Chang, Y.M.Wang, C.H.Lin, S.Y.Cheng. *Adv. Mater. Res.*, **702**, (2013); https://doi.org/10.4028/www.scientific.net/AMR.702.111
82. A.L.de Medeiros, A.E.Martinelli, D.M.de Araujo Melo, M.O.Orlandi, D.A.Macedo. *ECS Transactions*, **61**, 1 (2014); https://doi.org/10.1149/06136.0001ecst
83. L.B.Pinheiro, A.E.Martinelli, F.C.Fonseca. *Adv. Mater. Res.*, **975**, 154 (2014); https://doi.org/10.4028/www.scientific.net/AMR.975.154
84. S.Mago, K.L.Singh, A.P.Singh, C.Sharma, P.Sharma. *JOM*, **71**, 3796 (2019); https://doi.org/10.1007/s11837-019-03742-y
85. K.Li, J.Chen, J.Peng, R.Ruan, M.Omran, G.Chen. *J. Hazardous Mater.*, **384**, 121227 (2020); https://doi.org/10.1016/j.jhazmat.2019.121227
86. A.C.Chien, J.Y.Nicole. *Catal. Commun.*, **154**, 106312 (2021); https://doi.org/10.1016/j.catcom.2021.106312
87. J.Sacanell, M.G.Bellino, D.G.Lamas, A.G.Leyva. *Physica B-Condensed Matter*, **398** (2), 341 (2007); https://doi.org/10.1016/j.physb.2007.04.039
88. A.P.Khandale, S.S.Bhoga, R.V.Kumar. *Solid State Ionics*, **238**, 1 (2013); https://doi.org/10.1016/j.ssi.2013.02.010
89. J.Peng, J.Binner. *J. Mater. Sci. Lett.*, **21**, 247 (2002); https://doi.org/10.1023/A:1014781329612
90. I.Ganesh, R.Johnson, G.Rao, Y.Mahajan, S.Madavendra, B.Reddy. *Ceramics Int.*, **31**, 67 (2005); https://doi.org/10.1016/j.ceramint.2004.03.036
91. K.Tahmasebi, M.Paydar. *J. Alloys Compd.*, **509**, 4 (2011); https://doi.org/10.1016/j.jallcom.2010.09.176
92. .D.Punde, A.P.Khandale, S.S.Bhoga. *Solid State Ionics*, **262**, 701 (2014); https://doi.org/10.1016/j.ssi.2014.01.021
93. A.P.Khandale, B.S.Pahune, S.S.Bhoga, R.V.Kumar, R.Tomov. *Int. J. Hydrogen Energy*, **44**, 29 (2019); https://doi.org/10.1016/j.ijhydene.2019.04.055
94. N.H.Menzler, F.Tietz, S.Uhlenbruck, H.P.Buchkremer, D.Stöver. *J. Mater. Sci.*, **45** (2010); https://doi.org/10.1007/s10853-010-4279-9
95. S.A.M.Ali, M.Anwar, M.R.Somalu, A.Muchtar. *Ceramics Int.*, **43**, 4647 (2017); https://doi.org/10.1016/j.ceramint.2016.12.136
96. A.C.Ferrel-Alvarez, M.A.Dominguez-Crespo, H.Cong, A.M.Torres-Huerta, D.Palma-Ramirez, J.T.S.Irvine. *J. Alloys Compd.*, **851**, 156882 (2021); https://doi.org/10.1016/j.jallcom.2020.156882
97. Z.Yang, Y.Chen, C.Jin, G.Xiao, M.Han, F.Chen. *RSC Adv.*, **5**, 2702 (2015); https://doi.org/10.1039/C4RA11358F
98. W.Liu, H.Kou, X.Wang, L.Bi, X.Zhao. *Ceramics Int.*, **45**, 16 (2019); https://doi.org/10.1016/j.ceramint.2019.06.281
99. Z.Zhang, Y.Gong, D.Wu, Z.Li, Q.Li, L.Zheng, W.Chen, W.Yuan, L.Y.Zhang. *Int. J. Hydrogen Energy*, **44**, 5 (2019); https://doi.org/10.1016/j.ijhydene.2018.12.004
100. J.Mei, Y.Zhang, T.Liao, Z.Sun, S.X.Dou. *Nat. Sci. Rev.*, **5**, 3 (2018); https://doi.org/10.1093/nsr/nwx077
101. W.Gao, J.Sun, S.Liu, Y.Liu, C.Li, N.Tang. *J. Rare Earths*, **24**, 1 (2006); https://doi.org/10.1016/S1002-0721(07)60383-4
102. M.B.Choi, K.T.Lee, H.S.Yoon, S.Y.Jeon, E.Wachsman, S.J.Song. *J. Power Sources*, **220**, 15 (2012); https://doi.org/10.1016/j.jpowsour.2012.07.122
103. C.H.Hua, C.C.Chou. *Ceramics Int.*, **41**, S1 (2015); https://doi.org/10.1016/j.ceramint.2015.03.128
104. T.Saradha, A.Subramania, K.Balakrishnan, S.Muzhumathi. *Mater. Res. Bull.*, **68**, 320 (2015); https://doi.org/10.1016/j.materresbull.2015.03.071
105. F.J.A.Loureiro, D.A.Macedo, R.M.Nascimento, M.R.Cesario, J.P.F.Grilo, A.A.Yaremchenko, D.P.Fagg. *J. Eur. Ceramic Soc.*, **39**, 5 (2019); https://doi.org/10.1016/j.jeurceramsoc.2019.01.013
106. N.Ekraminejad, M.Jafari, T.Amiri, E.Shahsavari, H.Salamati, M.Ranjbar. *Mater. Chem. Phys.*, **278**, (2022); https://doi.org/10.1016/j.matchemphys.2021.125680